energyequipsys/ Vol 2/No2/AUG 2014/ 103-119

ENERGY EQUIPSYS

Energy Equipment and Systems

http://energyequipsys.ut.ac.ir
http://energyequipsys.com

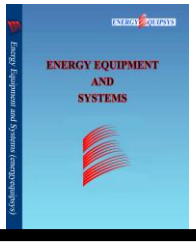

A numerical study on the effects of hydrogen addition levels, wall thermal conductivity and inlet velocity on methane/air pre-mixed flame in a micro reactor

Mohammadreza Baigmohammadi [a]
Sadegh Tabejamaat [a]*
Babak Kashir [a]

[a] Department of Aerospace Engineering, Amirkabir University of Technology (Tehran Polytechnic), Hafez Ave., Tehran, 15875-4413, Iran

Article history:

Received 21 April 2014
Accepted 17 July 2014

ABSTRACT

In this study, the effect of the levels of hydrogen addition to methane-air premixed flame in a micro-stepped reactor has been studied numerically. In addition, the effects of mixture velocity and walls' thermal conductivity (K_w) on the flame's location, temperature, and species distribution in a micro reactor were calculated using a 2D numerical laminar steady code. The results showed that an increasing level of hydrogen in the methane-air mixture probably improves the combustion process in a micro reactor by intensifying the flame speed, adiabatic flame temperature and the generation of some crucial species (such as OH, H, HCO, HO_2, and H_2O_2). Further, it was found that the addition of hydrogen to methane can shift the flame towards the inlet. In this way, it probably guarantees the flame's presence in certain conditions compared to cases of no hydrogen addition. In conclusion, it is shown that the temperature distribution along the axis and the wall of the micro reactor can be dependent on the amounts of hydrogen added to the methane-air mixture.

Keywords: Micro tube, Step, Methane, Air, Hydrogen, Reduced chemistry.

1. Introduction

Recently, the rate of scientific and industrial research into micro electromechanical systems (MEMS) including portable communication devices, micro robots, micro air vehicles and micro reactors has been expanding dramatically. These kinds of mechanical devices are small in size and low in weight. Therefore, finding a reliable, feasible, low-weight and cost effective source of energy is still one of the main obstacles hindering the development of this type of system. Currently, advanced chemical batteries are one of the options available to use in micro systems. They are large in size, low in their energy to weight ratio and have a short operation time. For these reasons, their usage in MEMS devices seems to be controversial. Therefore, other available sources of energy should be applied to provide the required energy in MEMS devices. Among the available sources of energy, hydrocarbon fuels, due to their high energy to weight density and also their low cost can also be recommended as a proper option for use in MEMS applications. In this respect, compatible reactors with MEMS conditions should be developed. Although applying the

*Corresponding author:
Department of Aerospace Engineering, Amirkabir University of Technology (Tehran polytechnic), Hafez Ave., Tehran, PO. Box: 15875-4413, Iran.
E-mail address: sadegh@aut.ac.ir (Sadegh Tabejamaat)

hydrocarbon fuels seems to be a remedy for providing enough energy in MEMS devices,their low combustion efficiency in micro scales is still a challenging matter. Therefore, a lot of research has been focused on developing meso or micro-scale reactors with adequate efficiency, in which the hydrocarbon fuels can be burnt properly [1,2,3,4,5,6].

The combustion process in a micro reactor can be affected by fuel type, the wall's thermal conductivity, the equivalence ratio, the inlet velocity, etc. Therefore, variations in the wall's thermal conductivity influence the heat recirculation process between the post-flame and pre-heating zones in the combustion field. The heat recirculation can control the combustion in meso and micro-scale reactors. Furthermore, the occurrence of unsteady and oscillatory flame modes under certain conditions in small-scale reactors has been reported in the literature. Norton and Vlachos (2003) showed that the flame presents oscillatory behaviour near the flame extinction limits. Moreover, according to the research by Maruta et al. (2005), the stable or unstable behaviour of a micro-flame depends largely on various parameters such as equivalence ratio, inlet mixture velocity, geometry, heat transfer conditions, micro-reactor wall temperature, and the incoming mixture's composition. Furthermore, they asserted that flame instability occurs at moderate velocity ranges. Thus, high or low enough inlet mixture velocities lead to stable flames, such as stable normal and weak flames, respectively.

In addition to the above mentioned topics, some approaches have been proposed by other researchers for improving combustion characteristics, such as flame location, temperature distribution, etc. in micro reactors. In this regard, Zarvandi et al. (2012) considered the effect of constant hydrogen addition to a methane-air mixture on the combustion process in a micro-scale reactor. They showed that adding hydrogen to a methane-air mixture can increase the flame strength against heat losses, as compared to the simple backward facing step reactor. In another research study conducted by Baigmohammadi et al. (2013), the effect of the insertion of conductive wire in a micro- increase flame strength against heat losses, although its effect on the flame is not as prominent as the hydrogen addition method.

Furthermore, the concept of a reverse-flow (RF) reactor has been studied numerically by Kaisare and Vlachos (2007). They proposed the reverse-flow operation as a remedy for extending the stabilized combustion zone due to the extra effect of pre-heating on combustion at the small-scale. Moreover, Federici and Vlachos (2008) conducted a numerical and experimental research study on the combustion stability of propane-air premixed flame in a heat recirculation micro channel. They found that the heat recirculation process via the wall of the reactor has a pivotal role in establishing a stable flame in a heat-recirculating burner. Furthermore, Ju and Choi (2003), and Kuo and Ronney (2007) have performed numerical research studies looking at the development of new methods for extending stable combustion operation in meso and micro-scale reactors. They investigated the dynamic and steady-state behaviour of excess enthalpy combustion in the two adjacent parallel channels with opposed flow direction and Swiss-roll reactors, respectively. They showed that a proper heat exchange between the two adjacent channels can extend the flame stability region in a micro reactor.

In this study, the effect of hydrogen addition levels on a methane-air mixture is studied numerically to improve methane-air pre-mixed flame characteristics such as the flame's location, temperature and species distributions, etc. in a micro-stepwise reactor. This approach has been studied in this work because of the remarkable effect of the addition of hydrogen on methane-air flame characteristics at meso or micro scales. Moreover, the usage of a hydrogen-air mixture at small scales seems to be challenging. Furthermore, this method has not yet been investigated adequately by other researchers in the micro-combustion field. Furthermore, the effects of inlet velocity and the reactor wall's thermal conductivity (K_w) on the flame's location, temperature distribution, and combustion progress in a micro-stepped reactor are simulated. For this purpose, a steady state modelling of the combustion has been performed using a high order, high accuracy 2D numerical code accompanied by a laminar pre-mixed fluid flow method.

Nomenclature

A	Area (m^2)
A_r	Pre-exponential factor

C_p	heat capacity at constant pressure (J/kg.K)
$C_{j,r}$	Molar concentration of species j in reaction r (kgmol/m^3)
D	mass diffusivity, m^2/s
e	Emissivity coefficient
E_r	Activation energy for reaction (J/kgmol)
h	specific enthalpy, J/kg
	Standard-state enthalpy (kJ/kgmol)
h_{out}	Outer wall convective heat transfer coefficient (W/m^2.K)
K	Thermal conductivity (W/m.K)
k_f	thermal conductivity of fluid or
or s	solid (W/m.K)
$k_{f,r}$	Forward rate constant for reaction r
$k_{b,r}$	Backward rate constant for reaction r
K_r	Equilibrium for the rth reaction
M_w	molecular weight, kg/mole
N	total number of chemical species
N_r	Number of reaction
p	Pressure (pa, p_{atm} = 101325 pa)
	Heat generation rate per unit of volume, W/m^3
r	Rate of reaction , kgmol/m^3.s
R_u	universal gas constant (R_u = 8313 J/(kg.kmol.K)
	Standard-state entropy (kJ/kgmol.K)
T	Temperature, K
u	x-direction velocity, m/s
v	y-direction velocity, m/s
	Stoichiometric coefficient of reactant species
	Stoichiometric coefficient of product species
x	Axial coordinate, m
k_{tr}	Monatomic value of thermal conductivity (W.m^{-1}.K^{-1})
φ	Property
y	Lateral directio, m
Y	mass fraction
β_r	Temperature exponent
μ	Dynamic viscosity, N.s/m^2
	Third body efficiency of the ith species in the rth reaction
ρ	Density, kg/m^3
σ	Lennard-Jones characteristic length, Angstroms
τ	Shear stress (Pa)
Ω_μ	Reduced collision integral
Ω_D	Analogous reduced collision integral
ω	species mass generation rate per unit volume
Γ	The net effect of third bodies on the reaction rate
	Ra e exponent for reactant species j in reaction r
	Rate exponent for product species j in reaction r

Subscript

exit	Outer surface of the reactor wall
i	species i th
i,m	species i in the mixture
ij	species i in species j th
in	Inlet
i,r	ith species in rth reaction
j	species j th
s	Solid
xx, yx, xy, yy	Tensor index
w	Wall
∞	ambient

2. Governing equations and numerical scheme

A schematic view of the simulated micro reactor is shown in Fig. 1a. As shown in this figure, methane/ hydrogen-air reactive mixtures with different mixing percentages enter the micro reactor. A reduced mechanism for methane-air combustion accompanied by 25 reversible reactions and15 species [15] (without N compositions) has been applied (Table 1). The equivalence ratio was set at 0.9 (lean mixture of methane-air) [16]. In this study, the inlet mixture temperature was 300 K. Furthermore, the wall's thermal conductivity, the added hydrogen mass fraction, and the inlet mixture velocities were varied from 3 to 90 W/m.K, 0.0 to 0.0258 and 2.8 to 11.8 m/s,

respectively. The hydrogen addition percentages have been chosen to show how increasing the hydrogen mass fraction in a methane/hydrogen-air mixture can improve the flame's stability inside the micro reactor. The reference outer wall convective heat transfer coefficient (h_{out}) of the micro reactorwas set at 5 $W/m^2.K$ [9,10,17]. Meanwhile, the radiative and convective heat transfer methods conveyed the generated heat energy in the combustion zone to the environment through the micro reactor outer wall. All the physical conditions of the modelling with the reference values of the thermal boundary conditions for the wall/ environmentinterfaces were summarized in Table 2. The dynamic viscosity and the thermal conductivity of the multi-components of the gas were calculated based on the methods presented in the references [18]. The lateral walls of the micro-reactor at the inlet and outlet were adiabatic.

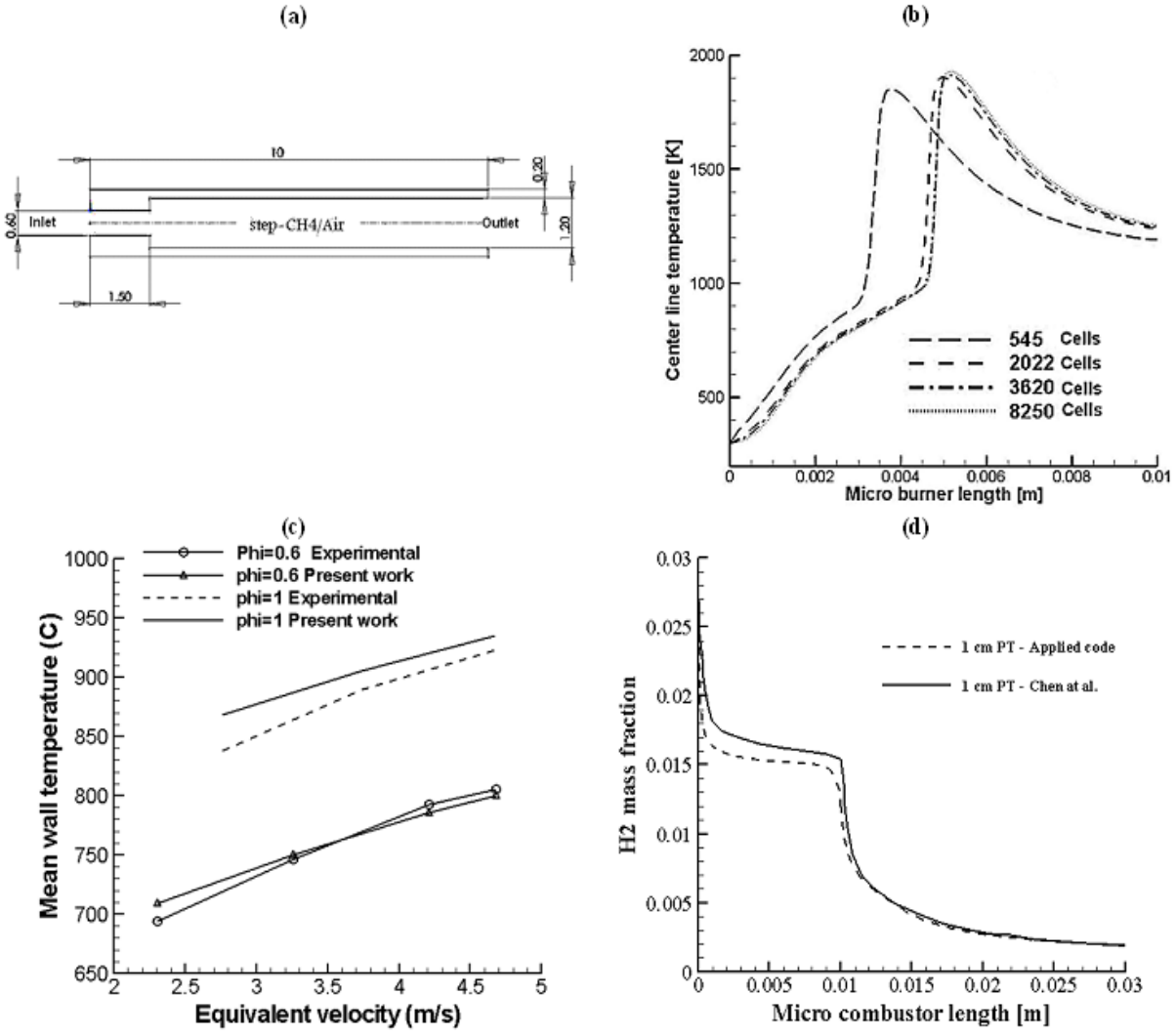

Fig. 1. (a) Dimension of a backward facing-step micro reactor (all dimensions are in mm), (b) the mesh study procedure (c,d) validation of the results of applied code by the results of (c) [19] and (d) [20]

Table 1. Skeletal mechanism for methane-air reaction

Rate constants are given in the form $k = A_k T^{\beta_k} \exp\left(-\frac{E_k}{R_u T}\right)$

Chemical Species

Total number of species: 17→ H, O_2, OH, O, H_2O, H_2, HO_2, H_2O_2, CO, CO_2, CH_4, CH_3, CH_2O, CH_3O, N, N_2, HCO

Label	Reaction	Ak (m,kmol,s)	βk	Ek (J/kmol)
1f	$H+O_2 \rightarrow OH+O$	2.E+11	0.00	7.034E+7
1b	$OH+O \rightarrow H+O_2$	1.575E+10	0.00	2.889E+6
2f	$O+H_2 \rightarrow OH+H$	1.800E+07	1.00	3.695E+07
2b	$OH+H \rightarrow O+H_2$	8.000E+06	1.000	2.830E+07
3f	$OH+H_2 \rightarrow H_2O+H$	1.170E+06	1.300	1.518E+07
3b	$H_2O+H \rightarrow OH+H_2$	5.090E+06	1.300	7.782E+07
4f	$OH+OH \rightarrow H_2O+O$	6.000E+05	1.300	0.00E+00
4b	$H_2O+O \rightarrow OH+OH$	5.900E+06	1.300	7.130E+07
5	$H+O_2+M \rightarrow HO_2+M^a$	2.300E+12	-0.800	0.000E+00
6	$HO_2+H \rightarrow OH+OH$	1.500E+11	0.000	4.204E+06
7	$HO_2+H \rightarrow H_2+O_2$	2.500E+10	0.000	2.931E+06
8	$HO_2+OH \rightarrow H_2O+O_2$	2.000E+10	0.000	4.187E+06
9f	$CO+OH \rightarrow CO_2+H$	1.510E+04	1.300	-3.174E+06
9b	$CO_2+H \rightarrow CO+OH$	1.570E+06	1.300	9.352E+07
10f	$CH_4(+M) \rightarrow CH_3+H(+M)^b$	6.300E+14	0.000	4.354E+08
10b	$CH_3+H(+M) \rightarrow CH_4(+M)^b$	5.200E+09	0.000	-5.485E+06
11f	$CH_4+H \rightarrow CH_3+H_2$	2.200E+01	3.000	3.663E+07
11b	$CH_3+H_2 \rightarrow CH_4+H$	9.570E-01	3.000	3.663E+07
12f	$CH_4+OH \rightarrow CH_3+H_2O$	1.600E+03	2.100	1.030E+07
12b	$CH_3+H_2O \rightarrow CH_4+OH$	3.020E+02	2.100	7.294E+07
13	$CH_3+O \rightarrow CH_2O+H$	6.800E+10	0.000	0.000E+00
14	$CH_2O+H \rightarrow HCO+H_2$	2.500E+10	0.000	1.671E+07
15	$CH_2O+OH \rightarrow HCO+H_2O$	3.000E+10	0.000	5.003E+06
16	$HCO+H \rightarrow CO+H_2$	4.000E+10	0.000	0.000E+00
17	$HCO+M \rightarrow CO+H+M$	1.600E+11	0.000	6.155E+07
18	$CH_3+O_2 \rightarrow CH_3O+O$	7.000E+09	0.000	1.074E+08
19	$CH_3O+H \rightarrow CH_2O+H_2$	2.000E+10	0.000	0.000E+00
20	$CH_3O+M \rightarrow CH_2O+H+M$	2.400E+10	0.000	1.206E+08
21	$HO_2+HO_2 \rightarrow H_2O_2+O_2$	2.000E+09	0.000	0.000E+00
22f	$H_2O_2+M \rightarrow OH+OH+M$	1.300E+14	0.000	1.905E+08
22b	$OH+OH+M \rightarrow H_2O_2+M$	9.860E+08	0.000	-2.123E+07
23f	$H_2O_2+OH \rightarrow H_2O+HO_2$	1.000E+10	0.000	7.536E+06
23b	$H_2O+HO_2 \rightarrow H_2O_2+OH$	2.860E+10	0.000	1.373E+08
24	$H+OH+M \rightarrow H_2O+M^a$	2.200E+16	-2.000	0.000E+00
25	$H+H+M \rightarrow H_2+M^a$	1.800E+12	-1.000	0.000E+00

a : Third body efficiencies: CH_4=6.5, H_2O=6.5, CO_2=1.5, H_2=1.0, CO=0.75, O_2=0.4, N_2=0.4, and all other species=1.0

b: Lindemann form, $k = \frac{k_\infty}{\left(1+\frac{k_{fall}}{[M]}\right)}$ where $k_{fall} = 6.3\exp\left(\frac{-7.536\times10^7}{R_u T}\right)$.

Table 2. The reference conditions

Model	2D-Axisymmetry-Reduced chemistry
Velocity or Mass Flow (u_{in} & $M_{dot,\ in}$)	2.8 m/s – 8.88e-7 kg/s
Thermal conductivity(Wall) (K_w)	20 W/m.K
External heat transfer coefficient (h_{out})	5 W/m^2.K
Emissivity coefficient (e)	0.2
Mass fraction of added hydrogen	0 - 0.0258
Equivalence ratio	0.9

The governing equations which are related to an axisymmetric, laminar steady state and a multi-species reactive flow are as follows [9,10]:

Continuity

$$\frac{\partial(\rho u)}{\partial x}+\frac{1}{r}\frac{\partial(\rho v r)}{\partial r}=0 \qquad (1)$$

Axial momentum

$$\frac{\partial(\rho u u)}{\partial x}+\frac{1}{r}\frac{\partial(\rho u v r)}{\partial r}= -\frac{\partial p}{\partial x}+\frac{\partial}{\partial x}\left(\frac{4}{3}\mu\frac{\partial u}{\partial x}\right)+\frac{1}{r}\frac{\partial}{\partial r}\left(r\mu\frac{\partial u}{\partial r}\right) -\frac{\partial}{\partial x}\left(\frac{2\mu}{3r}\frac{\partial(vr)}{\partial r}\right)+\frac{1}{r}\frac{\partial}{\partial r}\left(r\mu\frac{\partial v}{\partial x}\right) \qquad (2)$$

Viscosity

$$\mu_{mix}=\sum_i\left[\frac{x_i\mu_i}{\sum_j x_j\phi_{ij}}\right] \qquad (3)$$

$$\phi_{ij}=\frac{\left[1+\left(\frac{\mu_i}{\mu_j}\right)^{\frac{1}{2}}\left(\frac{M_j}{M_i}\right)^{\frac{1}{4}}\right]^2}{2\sqrt{2}\left(1+\frac{M_i}{M_j}\right)^{\frac{1}{2}}} \qquad (4)$$

Radial momentum

$$\frac{\partial(\rho u v)}{\partial x}+\frac{1}{r}\frac{\partial(\rho v v r)}{\partial r}= -\frac{\partial p}{\partial r}+\frac{\partial}{\partial x}\left(\mu\frac{\partial u}{\partial r}\right)-\frac{1}{r}\frac{\partial}{\partial r}\left(\frac{2r\mu}{3}\frac{\partial u}{\partial x}\right)+ \frac{\partial}{\partial x}\left(\mu\frac{\partial v}{\partial x}\right)+\frac{1}{r}\frac{\partial}{\partial r}\left(\frac{4r\mu}{3}\frac{\partial v}{\partial r}\right)-\frac{1}{r}\frac{\partial}{\partial r}\left(\frac{2}{3}\mu v\right) \qquad (5)$$

Energy equation

$$\frac{\partial}{\partial x}(\rho u h)+\frac{1}{r}\frac{\partial}{\partial r}(\rho v h r)= \frac{\partial}{\partial x}\left(k_f\frac{\partial T}{\partial x}\right)+\frac{1}{r}\frac{\partial}{\partial r}\left(k_f r\frac{\partial T}{\partial r}\right)+\dot{q} \qquad (6)$$

$$h=\sum_{i=1}^{N}Y_i h_i \qquad (7)$$

$$k_{mix}=\sum_i\left[\frac{x_i k_i}{\sum_j x_j\phi_{ij}}\right] \qquad (8)$$

$$\phi_{ij}=\frac{\varepsilon\left[1+\left(\frac{k_{tri}}{k_{trj}}\right)^{\frac{1}{2}}\left(\frac{M_j}{M_i}\right)^{\frac{1}{4}}\right]^2}{2\sqrt{2}\left(1+\frac{M_i}{M_j}\right)^{\frac{1}{2}}} \qquad (9)$$

In the above equation, according to [18],ε=1.0

$$\dot{q}=\sum_{i=1}^{N}\left(\frac{h_i^0}{M_i}+\int_{298.15}^{T}c_{p,i}dT\right)\omega_i \qquad (10)$$

$$\omega_i=M_i\sum_{i=1}^{N}\omega_{i,r} \qquad (11)$$

$$\omega_{i,r}=\Gamma\left(v''_{i,r}-v'_{i,r}\right)\left(k_{f,r}\prod_{j=1}^{N_r}\left[C_{j,r}\right]^{\eta'_{j,r}}-k_{b,r}\prod_{j=1}^{N_r}\left[C_{j,r}\right]^{\eta''_{j,r}}\right) \qquad (12)$$

$$k_{f,r}=A_r T^{\beta_r}\exp\left(-\frac{E_r}{R_u T}\right) \qquad (13)$$

$$k_{b,r}=\frac{k_{f,r}}{K_r} \qquad (14)$$

$$K_r = \exp\left(\underbrace{\frac{\Delta S_r^0}{R_u} - \frac{\Delta H_r^0}{R_u T}}_{Gibbs\,Free\,Energy}\right)\left(\frac{p_{atm}}{R_u T}\right)^{\sum_{i=1}^{N}\left(\nu''_{i,r}-\nu'_{i,r}\right)} \quad (15)$$

$$\frac{\Delta S_r^0}{R_u} = \sum_{i=1}^{N}\left(\nu''_{i,r}-\nu'_{i,r}\right)\frac{S_i^0}{R_u} \quad (16)$$

$$\frac{\Delta H_r^0}{R_u T} = \sum_{i=1}^{N}\left(\nu''_{i,r}-\nu'_{i,r}\right)\frac{h_i^0}{R_u T} \quad (17)$$

$$\Gamma = \sum_{j}^{N}\gamma_{j,r}C_j \quad (18)$$

Species conservation

$$\frac{\partial(\rho u Y_i)}{\partial x} + \frac{1}{r}\frac{\partial(\rho v r Y_i)}{\partial r} = \frac{\partial}{\partial x}\left[D_{i,m}\frac{\partial(\rho Y_i)}{\partial x}\right] + \frac{1}{r}\frac{\partial}{\partial r}\left[D_{i,m} r \frac{\partial(\rho Y_i)}{\partial r}\right] + \omega_i \quad (19)$$

Binary diffusivity

$$D_{ij} = 0.0188\frac{\left[T^3\left(\frac{1}{M_i}+\frac{1}{M_j}\right)\right]^{\frac{1}{2}}}{p\sigma_{ij}^2\Omega_D} \quad (20)$$

The energy equation in the wall of the micro reactor was formulated as follows:

$$\frac{\partial}{\partial x}\left[K_s\frac{\partial T_s}{\partial x}\right] + \frac{1}{r}\frac{\partial}{\partial r}\left[K_s r\frac{\partial T_s}{\partial r}\right] = h_{out}(T_s - T_\infty) + \sigma e(T_s^4 - T_\infty^4) \quad (21)$$

Finally, the various levels of the added hydrogen mass fraction have been calculated as follows:

$$AHMF = \frac{MFR\ of\ Added\ Hydrogen}{MFR\ of\ the\ Mixture\left(\left(CH_4 + H_2\right) + \left(Air\right)\right)} \quad (22)$$

where, AHMF and MFR are acronyms for Added Hydrogen Mass Fraction and Mass Flow Rate, respectively. The boundary conditions at the inlet and outlet of the micro reactor were the velocity inlet and pressure outlet, respectively [9,10]. Meanwhile, the internal fluid-wall radiative heat transfer interactions, the slip condition and the species diffusivity in the normal direction into the wall were ignored. The overall boundary conditions on the inner and outer sections of the micro reactor wall were as follows:

where

$$(x = 0\ and\ 0 \prec r \prec 0.3mm)$$

$$\rightarrow T = 300K, u = 2.8\,{}^{m}\!/_{s}, \nu = 0$$

$$\frac{\partial u}{\partial r} = 0, \frac{\partial \nu}{\partial r} = 0, \frac{\partial T}{\partial r} = 0, \frac{\partial Y_i}{\partial r} = 0$$

where

$$\left(0 < x < 1.5mm, r = 0.3mm\right) \rightarrow u = 0, v = 0\ {}^{m}\!/_{s}$$

where

$$\left(r = 0.8\ mm\right) \rightarrow q_{wall} = q_{exit}$$

where

$$\begin{pmatrix} x = 0,\ 0.3 < r < 0.8\,mm\ and \\ x = 10\,mm, 0.6 < r < 0.8\,mm \end{pmatrix} \rightarrow \frac{\partial T}{\partial x} = 0$$

The governing equations were solved by a finite-volume numerical scheme based on the SIMPLE (Semi-Implicit Method for Pressure Linked Equations) algorithm [9,10]. The non-dimensional convergence criterion for all the equations was 10^{-6}. As shown in Fig.1b, to find the best grid pattern in the flow field and the solid wall, a grid independency study was performed using several grids. Therefore, a computational grid with 5120 quad cells (3620 cells in the flow field zone and 1500 cells the in solid zone) was used [9,10].

With regard to the complexity of the computational procedures and the multi-aspect effects of the fluid flow parameters, reactions, and heat transfer, the results of this study have been verified using previously reported results [19,20]. As seen in Fig. 1c and d, the results of the applied computational scheme show an acceptable level of accuracy compared to the results of similar experimental and numerical works. Furthermore, the flame's location in this study is seen as the position with the highest temperature in the combustion field and at the centre of the reactor.

3. Results and discussion

The effects of different hydrogen addition levels, the wall's thermal conductivity and the inlet velocity on the behaviour of a methane-air premixed flame at micro scales are discussed below.

3.1 Effect of the wall's thermal conductivity

The effect of the wall's thermal conductivity

on the flame's location and characteristics in a micro reactor for the entrance mixture of methane/hydrogen-air of various compositions has been considered in this section. As seen in Fig. 2, adding hydrogen to the methane-air mixture can increase the adiabatic flame's temperature (Table 3), the laminar burning velocity, and simultaneously decrease the energy required to start ignition. According to the amount of hydrogen added to a methane-air mixture for the present cases ((H_2=0.01 & CH_4=0.031) and (H_2=0.0258 & CH_4=0.0)), it can be seen that higher amounts of hydrogen in the mixture can increase the adiabatic flame temperature and the laminar burning velocity (flame speed) of the free propagating flame. This increment can be nearly 2.5 and six times larger than the laminar burning velocity of the mixture of H_2=0.0 & CH_4=0.05, respectively. This can facilitate the initiation process of the reaction chain. As shown in Fig.3, the formaldehyde formation near the reactor inlet as a criterion for methane oxidation, heat release and combustion initiation is one of the main pieces of evidence for this effect [21,22,23].Therefore, it can be maintained that the early initiation of combustion has two opposite effects on the combustion process at micro-scales. In spite of there being several advantages to adding hydrogen to the methane-air mixture, if the flame is situated in a location very close to the inlet port, extra preheating by the reactor wall of the incoming mixture may be impaired. Therefore, this matter can lead to a significant decrease in the flame's temperature. This phenomenon can obviously be seen in Fig.2. Consequently, a desired flame with the required combustion characteristics may be acquired by adding hydrogen and locating the flame in a proper position at which the incoming mixture can be preheated properly.

Table 3. The adiabatic flame temperature and the flame speed of three (methane+ hydrogen)-air mixtures applied in this study

CH_4(mass fraction)	H_2(mass fraction)	Equivalence ratio	Flame speed (m/s)	Adiabatic flame temperature (K)
0.05	0.0	0.9	0.3488	~2120
0.041	0.005	0.9	0.5435	2140
0.031	0.01	0.9	0.7958	2170
0.0	0.0258	0.9	2.088	2240

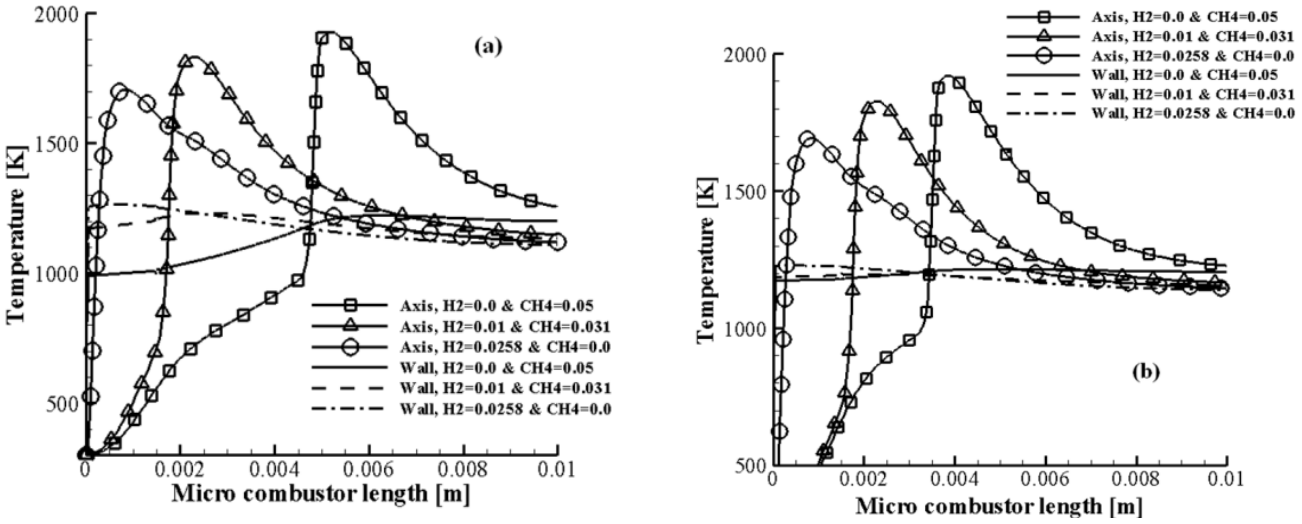

Fig. 2. Temperature distribution along the axis and next to the wall of micro reactor in the gas phase (wall) (a) Kw=20 W/m.K (b) Kw=90 W/m.K

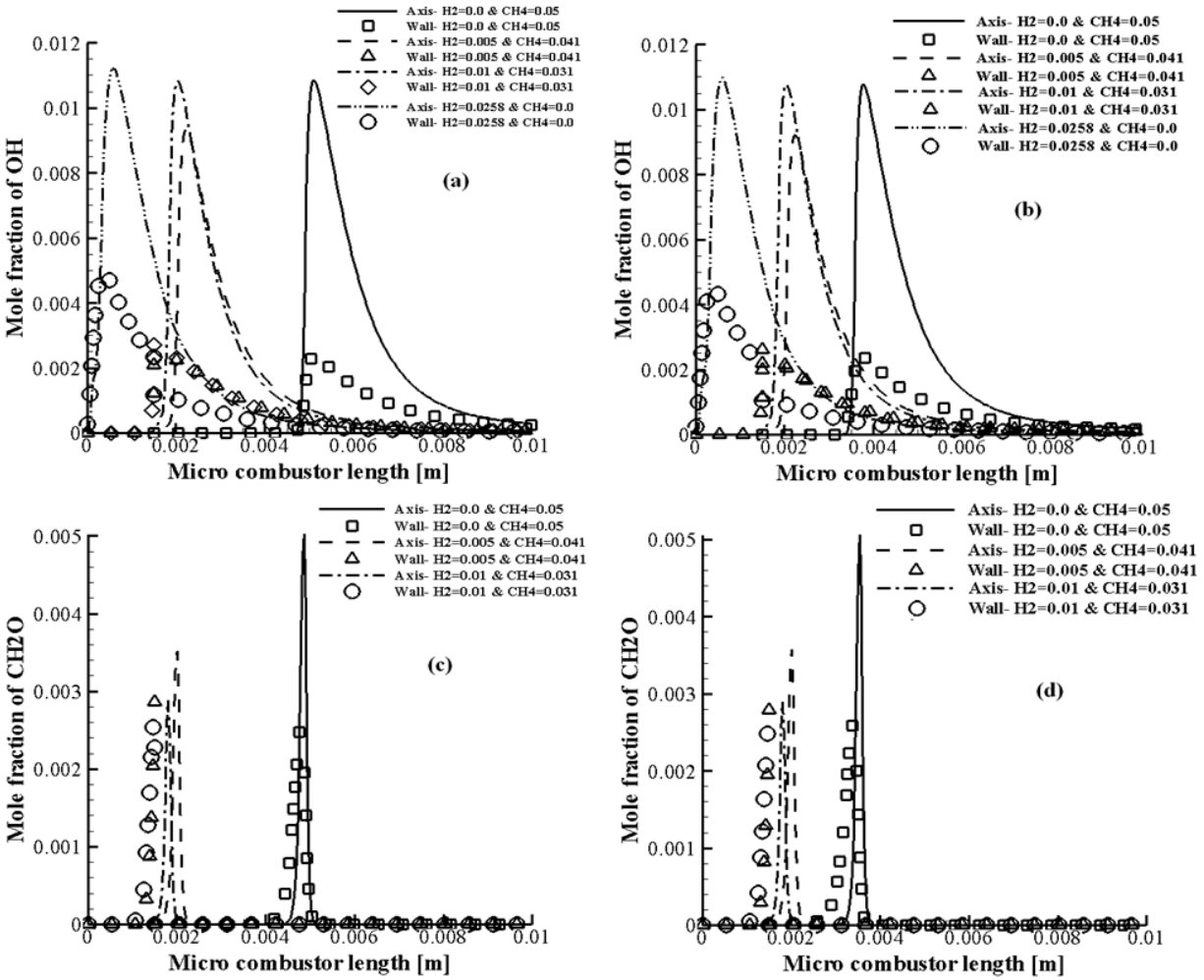

Fig. 3. Distribution of OH and CH2O along the reactor axis and next to the wall of micro reactor in the gas phase (wall) (a,c) Kw=20 W/m.K (b,d) Kw=90 W/m.K

Moreover, as shown in Fig. 2, variations in the wall's thermal conductivity cannot significantly influence the temperature distribution along the micro reactor axis using the hydrogen addition method in comparison to the non-hydrogen case. This behaviour can be attributed to the influence of the added hydrogen and the backward facing step, on the combustion and heat loss from the outer wall of the micro reactor. In this regard, the coincident effects of the added hydrogen and the backward facing step make the flame resistant against the increase of the wall's thermal conductivity. However, it should be noted that the effect of variation in the wall's thermal conductivity on the temperature distribution next to the wall of the micro reactor is significant.

Furthermore, the distributions of hydroxyl (OH) and formaldehyde (CH_2O) radicals along the axis and next to the wall of the micro reactor for two different wall thermal conductivities have been depicted in Fig. 3. The results revealed that the distributions of temperature next to the micro reactor wall and the radical pool near the wall have reciprocal effects on each other in all cases. It is clearly shown how adding hydrogen to the methane-air mixture shifts the hydroxyl and formaldehyde peak locations towards the inlet port and consequently stabilizes them at a position in the upstream. However, it should be noted that the distributions of hydroxyl and formaldehyde radicals near the reactor wall were slightly more sensitive to the wall's thermal conductivity in the hydrogen addition cases than those in the non-hydrogen addition case (Figs. 3a-d). Meanwhile, it can be inferred from Figs.3 a, b that adding hydrogen to the methane-air mixture by more than a critical amount can intensify the production of the "OH" radical as an active and prominent radical in the combustion field, especially near the wall. In this way, it can strengthen the flame's stability within the micro reactor. Moreover, adding hydrogen to the methane-air mixture not only can reduce the energy required to initiate the reactions, but can also intensify

the chain branching reactions which lead to methane and air (O_2+N_2) intermolecular bounds breaking. The levels of the generation of hydroxyl and formaldehyde can be presented as evidence of this matter. However, it should be noted that adding hydrogen to the methane-air mixture decreases the concentration of the carbon atoms. Therefore, the mole fraction of formaldehyde decreases based on the percent of hydrogen added to the methane-air mixture. However, some parameters such as the flame's location, the wall's temperature, chemical mechanisms, micro reactor diameter and the chemical composition of the incoming mixture can influence the distribution of OH radicals along the micro reactor.

Based on the results, the mass-weighted average mole fraction of the species has been used to obtain a proper understanding of the distribution of chemical species throughout the micro reactor. The applied definition of the mass-weighted average parameter has been presented in the research carried out by Zarvandi et al., 2012 and Baigmohammadi et al., 2013. In this regard, as shown in Fig. 4, adding hydrogen to the methane-air mixture can intensify the average mole fraction of some chemical species such as H, OH, H_2O, HO_2, H_2O_2, and HCO in the flow field more than those of the non-hydrogen addition case. Most of these species play the role of initiator and heat release markers for combustion in the micro reactor. Regarding Fig. 4, although variations in the wall's thermal conductivity influence the average mole fraction of some species in the micro reactor for both methods (the cases of hydrogen and non-hydrogen addition), its effect on the non-hydrogen addition case seems to be more distinctive [9].

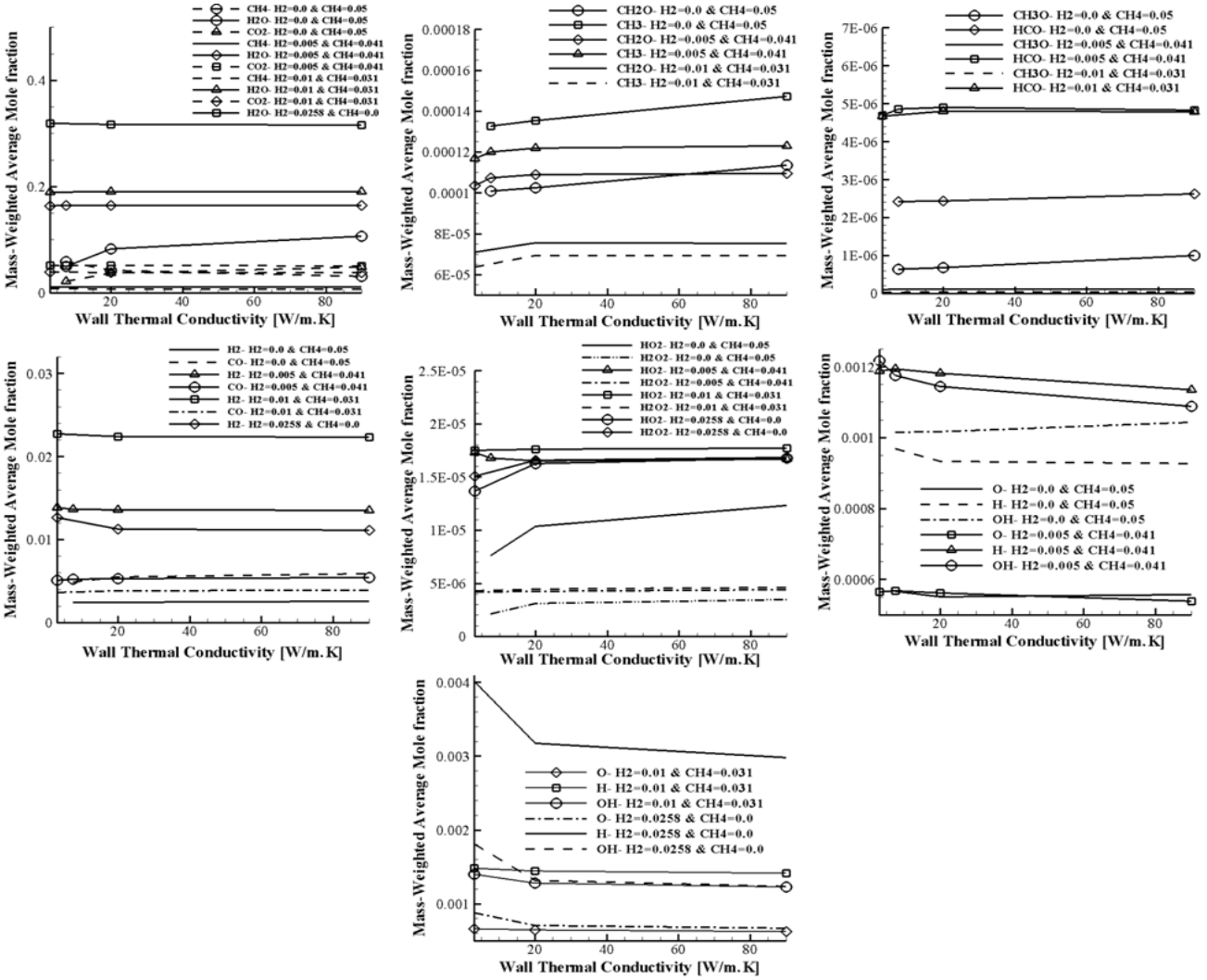

Fig. 4. Variations in the average value of species versus variations in the wall thermal conductivity coefficient for different values of hydrogen addition to methane-air mixture

Furthermore, Fig. 4 shows that the more the thermal conductivity of the wall increases the greater the average mole fraction of some species such as CH_3O, CO, HCO, CH_3, CH_2O, HO_2 and H_2O_2 becomes in the non-hydrogen addition case. However, variation of the wall's thermal conductivity has no major effect on the mass-weighted average mole fraction of some species in the hydrogen addition method. However, the increase of the wall's thermal conductivity can still decrease the mean mole fraction of the other species such as H, OH and O and also increases the mean mole fraction of CH_3 in the combustion field. The increase of the wall's thermal conductivity imposed this effect on the combustion field by increasing heat loss through the reactor wall. Therefore, during this process, H, OH and O can be counted as the vulnerable species in the combustion field.

Furthermore, the variation of the flame's location versus the wall's thermal conductivity for different levels of hydrogen addition is shown in Fig. 5. As shown, under such heat transfer conditions as mentioned in Table 2, increasing the amount of hydrogen added to the inlet reactive mixture makes the flame insensitive to variations in the wall's thermal conductivity. As depicted in Fig. 5, this insensitivity decreases as the level of hydrogen addition increases. Unlike the hydrogen/methane-air cases, the methane-air flame without hydrogen addition is very sensitive to variations in the wall thermal conductivity. Therefore, in the hydrogen addition cases, variations in the wall's thermal conductivity cannot affect the flame's location. This phenomenon probably occurred due to the effect of increasing the hydrogen addition on the laminar burning velocity (flame speed) of a determined mixture. Moreover, it can be related to the decreasing effect of hydrogen addition on the ignition activation energy and consequently the displacement of the flame towards the inlet port. On the whole, it can be maintained that the flame's sensitivity to variations of the wall's thermal conductivity can be decreased by adding sufficient hydrogen to the methane-air mixture.

3.2 Effect of inlet velocity

As depicted in Figs. 6 and 7, increasing the inlet velocity influences the flame's location, the distributions of temperature and species, along the centre line and next to the wall of the micro reactor in the gas phase. In such conditions as this of the inlet mixture velocity, the flame without hydrogen addition cannot be sustained inside the micro reactor. This behaviour seems to depend on the combustion nature which takes place in the micro reactor. As seen in Figs. 7 a-b, increasing the inlet mixture velocity reduces the flow time scale compared to the reaction time scale. Therefore, the flame location moves towards the downstream of the reactor. Moreover, as shown in Figs. 7 c-d, the increase of inlet velocity has a great influence on the formaldehyde distribution and its peak values along the axis of the micro reactor for various levels of hydrogen

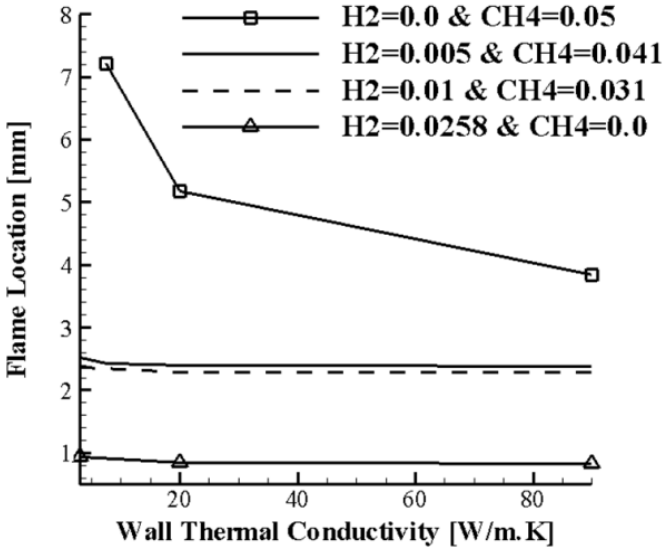

Fig. 5. Variations in the flame location versus the wall thermal conductivity for different values of hydrogen addition to methane-air mixture

addition. By comparing Fig. 7c with Fig. 7d, it can be inferred that the increase of inlet mixture velocity pushes the flame's location slightly towards the outlet. However, by increasing the wall's temperature and also the flame's stretching at the centre, the peak value of the formaldehyde distribution near the wall will be more than its peak value on the axis. Furthermore, it is seen that an increase of the inlet velocity from 2.8 m/s to 11.8 m/s changes the peak values of the formaldehyde next to the wall, so that, unlike Fig. 7c, the peak value of formaldehyde in the case of (H_2: 0.01 and CH_4: 0.031) is more than its value in the case of (H_2: 0.005 and CH_4: 0.041).

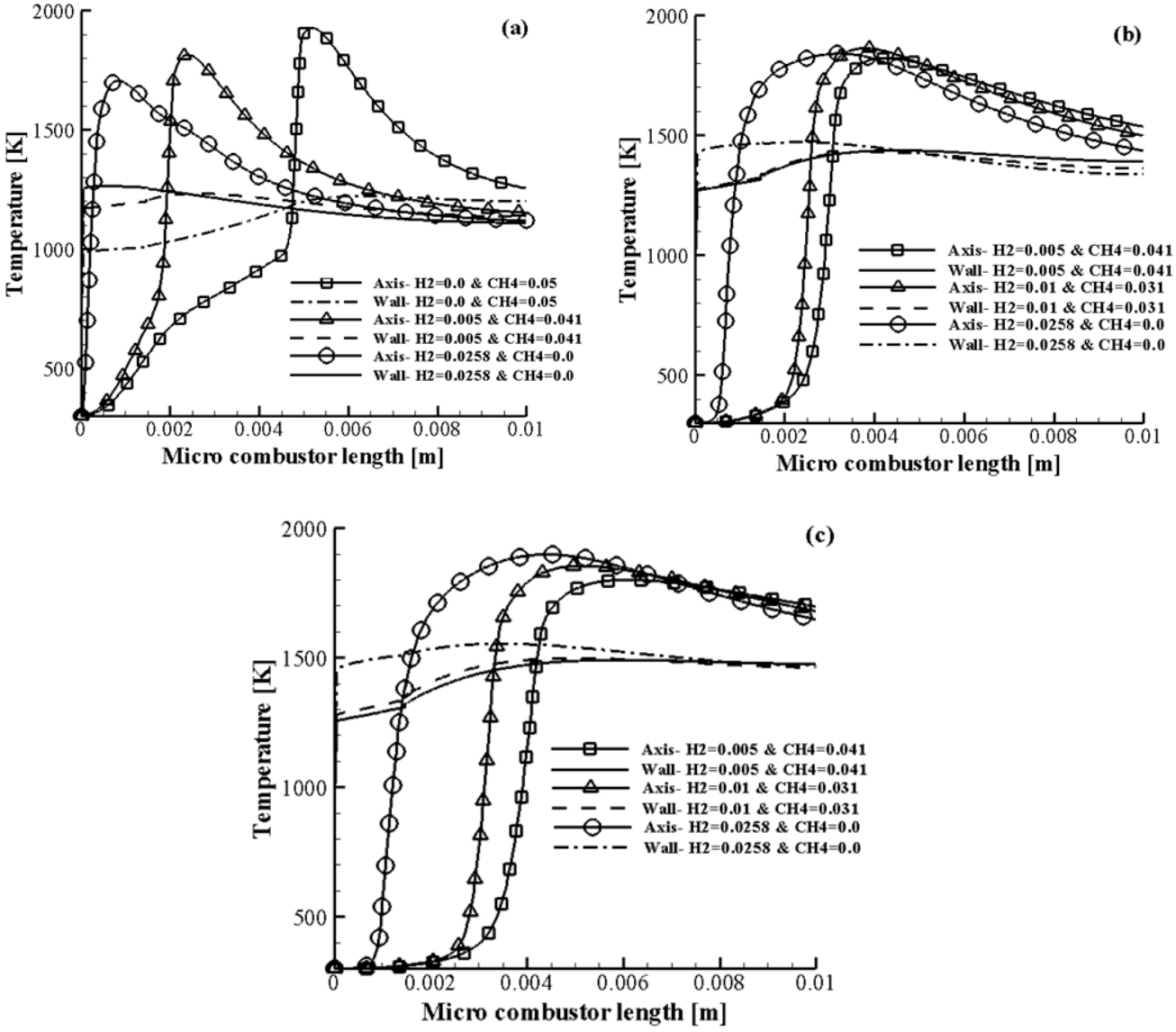

Fig. 6. Temperature distribution along the axis and next to the wall of micro reactor in the gas phase (wall) (a) Vin=2.8 m/s (b) Vin=7.8 m/s (c) Vin=11.8 m/s

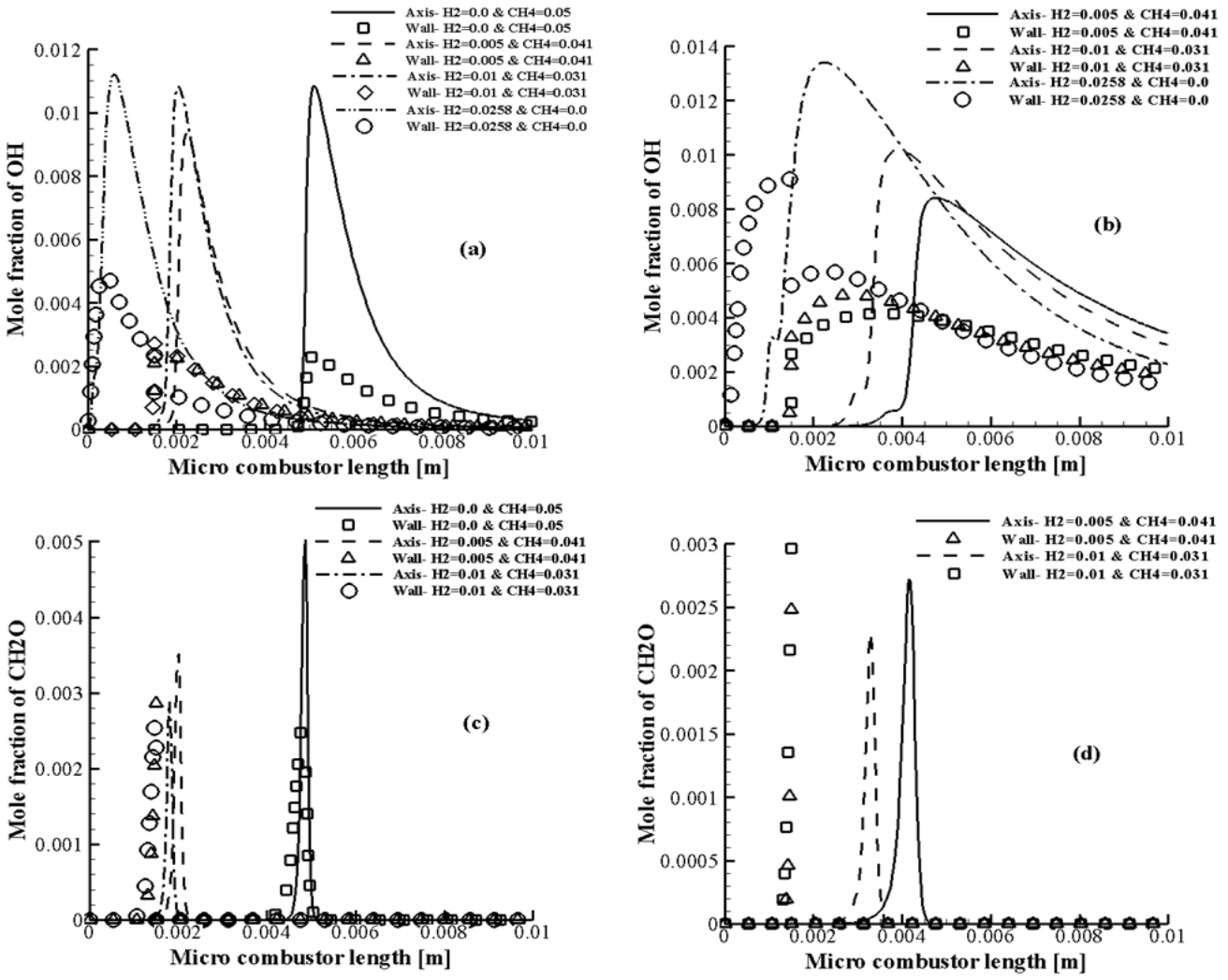

Fig. 7. Distribution of OH and CH2O along the reactor axis and next to the wall in the gas phase (wall) (a,c) Vin=2.8 m/s (b,d) Vin=11.8 m/s

Furthermore, it is known that at the constant equivalence ratio and flame speed, increased incoming premixed reactive flow brings more heating energy to the combustion zone. This matter can be intensified by increasing the heating value, the adiabatic flame temperature and the flame speed of the reactive mixture. In contrast, increasing the reactive mixture velocity by much more than the flame speed can push the flame towards the reactor outlet. Therefore, as shown in Fig. 8, an increase of the inlet mixture velocity can increase the mass weighted average of the mole fraction of the various species such as CH_4, OH, H, O, CH_2O, CH_3, H_2, CO, H_2O_2, HO_2, HCO and simultaneously decrease the mass weighted average of the mole fraction of the other species such as H_2O, CO_2, CH_3O in the combustion zone of the micro reactor. These increasing and decreasing trends are strongly dependent on the hydrogen addition level in the incoming reactive mixture. Furthermore, increased heating of the micro reactor wall can occur (Fig. 6) due to a proper increase of the entrance mixture velocity which can intensify the combustion heat release rate in the micro reactor. Moreover, this is due to the fact that increasing the inlet mixture velocity moves the flame's location towards the outlet. Therefore, the simultaneous effects of a higher heat release rate and flame displacement can provide a suitable opportunity for increased preheating of the fresh incoming mixture before it enters the flame zone. Increased preheating can increase the flame temperature and also the dissociation intensity of the chemical species in the flame zone. Furthermore, due to the dependence of the species dissociation rate on the flame temperature and the heat loss, the increase of flame temperature leads to a

higher mean mole fraction of some chemical radical species inside the micro reactor.

On the other hand, as seen in Fig. 8, an increase of the entrance mixture velocity increases the mean mole fraction of CH_4, H_2, and CO. This leads to a decreasing trend in the mean mole fraction of H_2O and CO_2. The phenomenon shows that increasing the inlet mixture velocity can disturb the fuel conversion process and this makes the flame prone to going out. However, increasing the hydrogen addition level in the incoming mixture can properly compensate for this status by increasing the adiabatic flame temperature and the flame speed.

Furthermore, as depicted in Fig. 9, an increase in the incoming mixture velocity pushes the flame's location towards the reactor outlet for the all the hydrogen addition levels. As seen in this figure, by increasing the amount of hydrogen, the flame's resistanceagainst the blowout has been increased dramatically. However, in the non-hydrogen addition case, the flame can be established in only a very narrow band of the incoming mixture velocities in the reactor. Therefore, it can be concluded that reducing the reaction time scale by adding hydrogen to the methane-air mixture and the low heat losses are the two main reasons for the phenomenon. This confirms that although using hydrogen in the micro reactors as a source of fuel may impose some storage difficulties on the system, its use as an additive with a methane-air reactive mixture can compensate for the storage problem and also increases the combustion efficiency in the micro reactors.

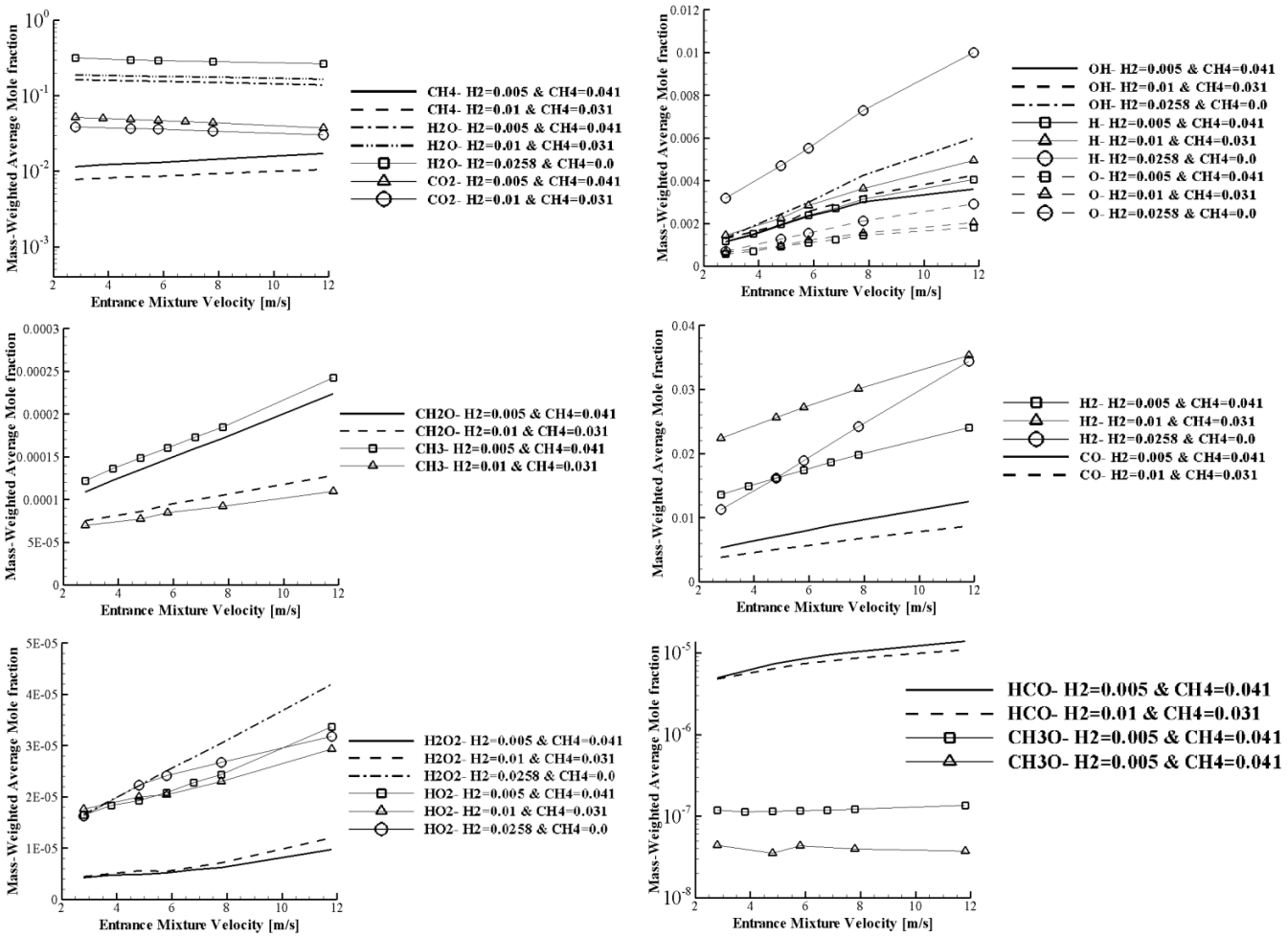

Fig.8. Variation in the average value of species versus variations in the incoming mixture velocity for different levels of hydrogen addition to methane-air mixture

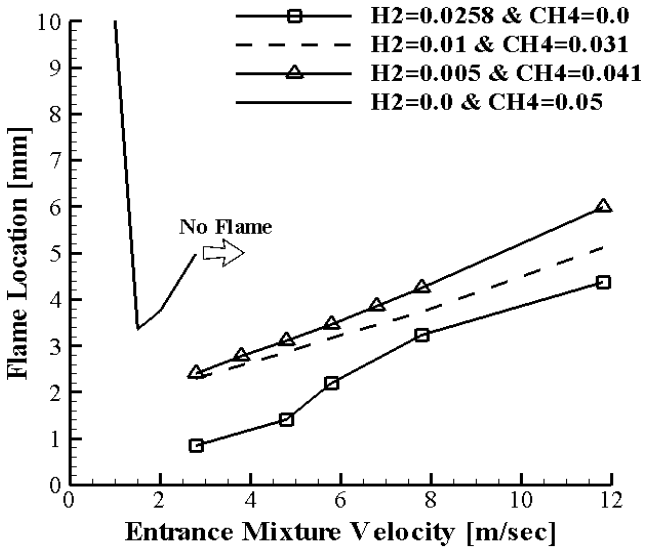

Fig. 9. Variation in the flame location versus the entrance mixture velocity for different levels of hydrogen addition to methane-air mixture

4. Conclusions

In this study, the effect of various levels of hydrogen addition on the methane-air mixture for improving its premixed combustion in a micro reactor has been studied numerically. The effects of entrance mixture velocity and the reactor wall's thermal conductivity (K_w) on the flame's location, temperature distribution, and the combustion progress in a micro-stepped reactor were calculated using a two dimensional laminar pre-mixed steady-state numerical code. It was shown that by increasing the wall's thermal conductivity in the absence of rigorous radiative and convective heat losses from the outer wall, the flame can be established in a location close to the inlet. Furthermore, it was found that although increasing the wall's thermal conductivity has an obvious effect on the flame's location, temperature distribution, and the mean mole fraction of the chemical species in the non-hydrogen addition case, its effect on these parameters in the cases with hydrogen addition seemed to be inconspicuous. The numerical results showed that the addition of hydrogen to the methane-air mixture can intensify the production of some crucial species such as OH, H, HCO, O, HO_2, and H_2O_2 which are vital for establishing stable combustion inside the micro reactor. Furthermore, the incoming mixture velocity can impressively influence the flame's location, temperature distribution and the mean mole fraction of the chemical species in the micro reactor. Based on the presented results, it appears that decreasing the flow time scale, rather than the chemical reaction time scale, increases the incoming velocity and can push the flame location towards the reactor outlet. Therefore, the simultaneous usage of a suitable percentage of added hydrogen to the methane-air mixture and higher inlet velocities which can lead to higher wall temperatures, influence the flame's location and the temperature distribution in the micro reactor. However, as seen previously, by increasing the amount of hydrogen which can be added to the methane-air mixture, the flame's resistance against blowing out increased dramatically. In the non-hydrogen and low hydrogen addition cases, the flame can only be established in a very narrow band of the incoming mixture of velocities in the reactor. This matter may occur due to an increasing effect of the addition of hydrogen on the adiabatic flame's temperature and the flame's speed. In this way, the combustion's efficiency in the micro reactor can be increased. On the whole, it can be maintained that the proper use of hydrogen addition to the methane-air mixture was adequately eligible and a recommendable approach which can be applied to the micro reactors especially for time-restricted micro combustion systems.

Acknowledgements

The authors would like to show their thanks to Dr. Samaneh E. Tousi for her help in the preparation of the paper.

Conflict of Interest

There is no conflict of interest. Furthermore, the authors declare there are no competing financial interests.

References

[1] Jejurkar, S.Y., Mishra, D.P.: A review of recent patents on micro-combustion and applications. Recent Pat Eng. 3, 194-209, 2009.

[2] Kaisare, N.S., Vlachos, D.G.: A review on micro combustion: Fundamentals, devices and applications. Prog Energ Combust. 38, 321-359, 2012.

[3] Chia, L.C., Feng, B.: Review; The development of a micro power (micro-thermo photovoltaic) device. J Power Sources. 165, 455-480, 2007.

[4] Walther, D.C., Ahn, J.: Advances and challenges in the development of power generation systems at small scales. Prog Energ Combust. 37, 583-610, 2011.

[5] Maruta, K.: Micro and meso scale combustion. Proc Combust Inst. 33, 125-150, 2011.

[6] Ju, Y., Maruta, K.: Microscale combustion: Technology development and fundamental research, Prog Energ Combust. 37, 669-715, 2011.

[7] Norton, D.G., Vlachos, D.G.: Combustion characteristics and flame stability at the micro scale: a CFD study of premixed methane/air mixtures. Chem. Eng. Sci. 58, 4871-4882, 2003.

[8] Maruta, K., Kataoka, T., Kim, N.I., Minaev, S., Fursenko, R.: Characteristics of combustion in a narrow channel with a temperature gradient. Proc. Combust. Inst. 30, 2429-2436, 2005.

[9] Zarvandi, J., Tabejamaat, S., Baigmohammadi, M.: Numerical study of the effects of heat transfer methods on CH_4/ (CH_4 +H_2)-Air pre-mixed flames in a micro-stepped tube. Energy. 44, 396-409, 2012.

[10] Baigmohammadi, M., Sarrafan Sadeghi, S., Tabejamaat, S., Zarvandi, J.: Numerical study of the effects of wire insertion on CH_4 (methane)/Air pre-mixed flame in a micro reactor. Energy. 54(1), 271-284, 2013.

[11] Kaisare, N.S., Vlachos, D.G.: Extending the region of stable homogeneous micro-combustion through forced unsteady operation. Proc. Combust. Inst. 31, 3293-3300, 2007.

[12] Federici, J . A . , Vlachos, D . G . : A computational fluid dynamics study of propane/air micro flame stability in a heat recirculation reactor. Combust. Flame. 153, 258-269, 2008.

[13] Ju, Y., Choi, C.W.: An analysis of sub-limit flame dynamics using opposite propagating flames in mesoscale channels. Combust. Flame. 133, 483-493,2003.

[14] Kuo, C.H., Ronney, P.D.: Numerical modeling of non-adiabatic heat-recirculating reactors. Proc. Combust. Inst. 31, 3277-3284, 2007.

[15] Smooke, M.D., Giovangigli, V.: Formulation of the premixed and non-premixed test problems, in reduced kinetic mechanisms and asymptotic approximations for Methane-Air flames, in: Araki, H., Brezin, E., Ehlers, J., Frisch, U., Hepp, K., Jaffe, R.L., Kippenhahn, R., Weidenmuller, H.A., Wess, J., Zittartz, J. (Eds.), Modeling in Combustion Science, Springer-Verlag, Berlin, pp. 1-28, 1991.

[16] Cao, H.L., Xu, J.L.: Thermal performance of a micro-reactor for micro-gas turbine system. Energ. Convers. Manage. 48, 1569-1578, 2007.

[17] Evans, C.J., Kyritsis, D.C.: Operational regimes of rich methane and propane/oxygen flames in mesoscale non-adiabatic ducts. Proc. Combust. Inst. 32, 3107-3114, 2009.

[18] Poling, B.E., Prausnitz, J.M., O'Connell, J.P.: The properties of gases and liquids, fifth ed. McGraw –Hill, pp. 9-15, 2001.

[19] Li, J., Chou, S.K., Li, Z.W., Yang, W.M.: Characterization of wall temperature and radiation power through cylindrical dump micro-reactors. Combust. Flame. 156, 1587-1593, 2009.

[20] Chen, G.B., Chao, Y.C., Chen, C.P.: Enhancement of hydrogen reaction in a micro-channel by catalyst segmentation. Int. J. Hydrogen Energ. 33, 2586-2595, 2008.

[21] Gordon, R., Masri, A., Mastorakos, E.: Heat release rate as represented by [OH] × [CH_2O] and its role in autoignition. Combust. Theor. Model. 13(4), 645-670, 2009.

[22] Vasudevan, V., Davidson, D.F., Hanson, R.K., Bowman, C.T., Golden, D.M.: High-Temperature measurements of the rates of the reactions CH_2O+Ar products and CH_2O+O_2 products. Proc. Comb. Inst. 31, 175-183, 2007.

[23] Vasudevan, V., Davidson, D.F., Hanson,

R.K.: Direct measurements of the reaction $OH+CH_2O \rightarrow HCO+H_2O$ at high temperatures. Int. J. of Chem. Kinetics. 37, 98-109, 2005.